Optical loss analysis of monolithic perovskite/Si tandem solar cell

Citation: Mailoa, Jonathan P., et al. "Optical Loss Analysis of Monolithic Perovskite/Si Tandem Solar Cell." 2015 IEEE 42nd Photovoltaic Specialist Conference (PVSC), IEEE, 2015, pp. 1–3. © 2015 IEEE

As Published: http://dx.doi.org/10.1109/PVSC.2015.7356420

Publisher: Institute of Electrical and Electronics Engineers (IEEE)

Persistent URL: http://hdl.handle.net/1721.1/119162

Version: Author's final manuscript: final author's manuscript post peer review, without publisher's formatting or copy editing

Optical Loss Analysis of Monolithic Perovskite/Si Tandem Solar Cell

Jonathan P. Mailoa[1], Colin D. Bailie[2], Austin J. Akey[1], Eric T. Hoke[2], Eric C. Johlin[1], William H. Nguyen[2], Sarah E. Sofia[1], Michael D. McGehee[2], and Tonio Buonassisi[1]

[1]Massachusetts Institute of Technology, Cambridge, MA 02139, USA
[2]Stanford University, Stanford, CA 94305, USA

***Abstract* — Coupling perovskite and silicon solar cells in a tandem configuration is considered an attractive method to increase conversion efficiency beyond the single-junction Shockley-Queisser limit. While a mechanically-stacked perovskite/silicon tandem solar cell has been demonstrated, a method to electrically couple perovskite and silicon solar cell in a monolithic configuration has not been demonstrated. In this contribution, we design and demonstrate a working monolithic perovskite/silicon tandem solar cell, enabled by a silicon tunnel junction, with a V_{OC} of 1.58 V. We further discuss possible efficiency loss mechanisms and mitigation strategies.**

***Index Terms* — multijunction solar cells, perovskite solar cells, silicon, tandems, tunnel junction.**

I. Introduction

In the last 25 years, the efficiency of silicon solar cells has only increased by less than 1.0% absolute. To achieve further improvements to silicon device efficiency, tandem approaches are considered. In particular, a perovskite/silicon tandem solar cell reduces the thermalization loss and offers a possible pathway to exceed the current silicon solar cell record efficiencies while making use of the low-cost, high-bandgap perovskite material as the top cell. We have previously demonstrated a working mechanically-stacked perovskite/silicon tandem cell [1]. However, to demonstrate a working monolithic perovskite/silicon tandem, development of a suitable recombination interlayer is necessary.

We develop a monolithic perovskite/silicon tandem solar cell using a silicon tunnel junction built directly on top of the silicon bottom cell emitter while taking advantage of the conduction band alignment between the silicon tunnel junction and the perovskite electron selective contact (TiO_2) [2]. This enables efficient carrier transport from the perovskite cell into the bottom silicon cell. Our best monolithic tandem cell to date has an open-circuit voltage (V_{OC}) of 1.58 V, which is approximately the V_{OC} sum of the two sub-cells in the tandem, an efficiency of 13.7%, and an active device area of 1 cm^2.

II. Experimental Result and Discussion

A. Bottom Silicon Cell Design

We design our bottom silicon cell to be compatible with perovskite solar cell deposition/process flow. This means the silicon cell is designed such that perovskite cell deposition can be made on the cell in the same way a perovskite cell is being made on an FTO-coated glass. These design decisions have a few consequences: (1) To minimize chances of perovskite cell shunting during semi-transparent top contact deposition (Ag nanowire lamination procedure used in [1]), the bottom silicon cell is made to have a planar top surface; (2) To ease electron transfer from the perovskite TiO_2 layer, it is ideal to use a tunnel junction material with a conduction band well aligned to TiO_2, for which crystalline silicon is a suitable candidate; (3) To prevent the perovskite from decomposing due to high temperature, any high-temperature processes, including back metallization and chemical protection of such metal, has to be done before the perovskite cell deposition.

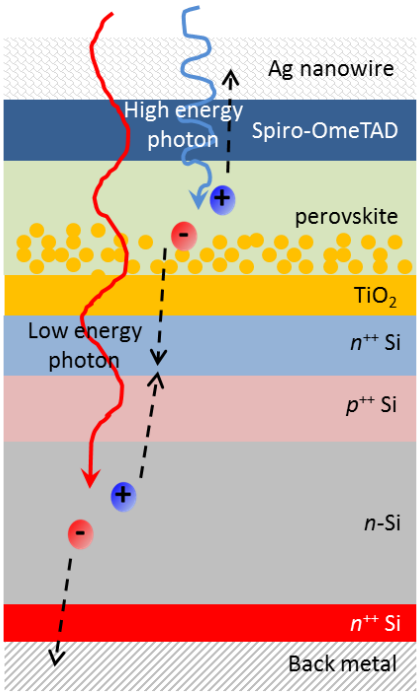

Fig. 1. Charge recombination mechanism in the monolithic perovskite/silicon tandem cell interlayer. Holes in the p^{++} emitter diffusing in from the n-type bulk silicon recombine with electrons in the n^{++} silicon layer arriving from the perovskite cell's electron selective contact (TiO_2) adjacent to the n^{++}/p^{++} silicon interface.

After employing these design decisions on the *n*-type bottom silicon cell, the likely charge recombination mechanism in the perovskite/silicon interlayer is shown in Fig. 1. To make the bottom silicon cell, we first start with a double-side polished

<100> n-type float zone silicon wafer (1–5 Ω·cm, 300 μm thickness). We protect the top side of the wafer by silicon nitride (SiN_x) protection, and then texture the bottom side of the cell using potassium hydroxide (KOH) solution. After removing the SiN_x protective layer using hydrofluoric acid (HF), the p^{++} emitter and the n^{++} back surface field (BSF) are formed by implanting boron on the planar top surface (^{11}B with 1.8×10^{15} cm^{-2} dose, 7 keV implantation energy) and phosphorus on the textured back surface (^{31}P with 4×10^{15} cm^{-2} dose, 10 keV implantation energy), followed by 960°C drive-in anneal in an N_2 ambient for 30 minutes.

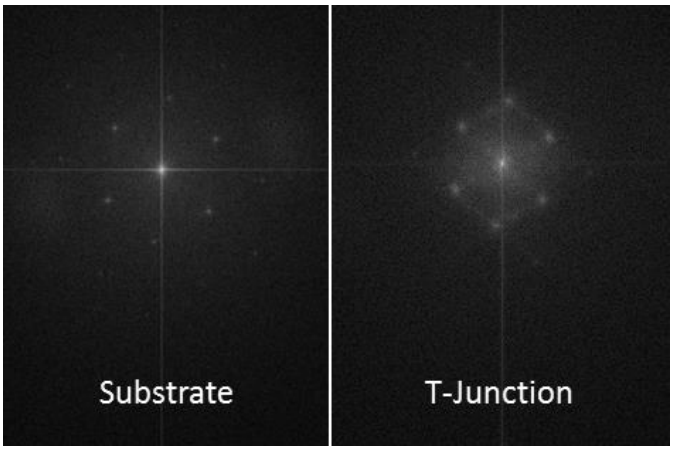

Fig. 2. Diffraction pattern of the partially crystallized n^{++} silicon tunnel junction layer and its underlying silicon substrate.

The n^{++} tunnel junction layer is then deposited using plasma-enhanced chemical vapor deposition (PECVD). The 30 nm-thick n^{++} layer is initially amorphous. The amorphous silicon is not ideal because in addition to having lower active dopant concentration (not ideal for tunnel junction formation) than crystalline silicon, its conduction band is also not well aligned to TiO_2 (TiO_2 conduction band is aligned to crystalline silicon) [3]. Because of this, we partially crystallize the amorphous silicon layer using rapid thermal anneal (680°C anneal in N_2 ambient for 15 minutes). The resulting n^{++} silicon layer is partially crystalline, as we have previously shown using transmission electron microscopy (TEM) [2]. This annealing temperature is used to enable partial crystallization of amorphous silicon while maintaining low dopant interdiffusion across the tunnel junction. The resulting tunnel junction doping profile has a doping concentration of 10^{19}–10^{20} cm^{-3} on both sides of the p^{++}/n^{++} interface, as shown by secondary ion mass spectroscopy (SIMS) [2], which is desired for tunnel junction formation.

To further investigate how the tunnel junction layer was formed, we look at the TEM diffraction pattern of the partially crystallized silicon tunnel junction layer as shown in Fig. 2. The diffraction pattern shows clear sign of the tunnel junction layer's crystallinity. When compared with the diffraction pattern of the underlying silicon substrate, we notice that the diffraction pattern of the tunnel junction is more blurry, indicating that the tunnel junction layer is indeed only partially crystalline. Nevertheless, one interesting observation is that the crystal orientation of the tunnel junction layer is identical to that of the underlying substrate, which suggests that the crystallization of the amorphous layer happens through solid phase epitaxy, with the underlying crystalline silicon substrate serving as the template for crystal growth.

After forming the tunnel junction on top of the n-type cell, we proceed to complete the monolithic perovskite/silicon tandem solar cell. We deposit the metal back contact stack (Ti/Pd/Ag/Pt, 20/20/300/30 nm) using electron beam evaporation and rapid thermal anneal (400°C anneal in an N_2 ambient for 5 minutes) to improve metal adhesion, with the Pt layer to be used as the corrosion-protection layer during subsequent perovskite cell deposition.

We then deposit a 30-nm thick layer of TiO_2 using atomic layer deposition (ALD, substrate temperature 150°C, TDMAT precursor temperature 80°C, and N_2 carrier gas at 20 sccm). TiO_2 residue (from ALD) sticking on the back metal of the cell is removed using dilute HF. Finally, the rest of the perovskite cell layers (with $CH_3NH_3PbI_3$ methyl-ammonium lead iodide perovskite blend absorber) from the spin-coated mesoporous TiO_2 layer to the Ag nanowire lamination layer is deposited on top of the tunnel junction cell, making a complete monolithic perovskite/silicon tandem solar cell stack.

B. Cell Measurement Results and Optical Loss Analysis

The *J-V* curve of the cell is measured under AM1.5G illumination. The data points are taken with 100 mV voltage steps, measured after each voltage steps has settled down for 5 s [2]. Based on this measurement, we determined that the maximum power point voltage V_{MPP} is close to 1.2 V. Steady-state measurements are then performed on the device to determine the stable device performance, shown in Table 1.

J_{SC}	11.5 mA/cm^2
V_{OC}	1.58 V
J_{MPP}	11.4 mA/cm^2
V_{MPP}	1.2 V
η	13.7%
FF	0.75

Table 1. Stable monolithic perovskite/silicon tandem cell device performance.

Based on the *J-V* curve, we know that the main limiting factor for the performance of our current tandem device is the J_{SC} of the cell, which is only ~11.5 mA/cm^2. Based on preliminary external quantum efficiency (*EQE*) measurements, the tandem is current-limited by the short circuit current in the top perovskite cell [2]. Normally the perovskite cell is illuminated from the TiO_2 side (n-side illumination), and is capable of reaching J_{SC} of up to 19.5 mA/cm^2 [4]. However, in this architecture the perovskite is being illuminated from the

perovskite hole selective contact layer (Spiro-OMeTAD, or the *p*-side). In addition to the parasitic absorption loss, the perovskite cell also loses some photocurrent due to low collection efficiency for photocurrent generated in the solid perovskite overlayer on top of the mesoporous TiO_2 layer.

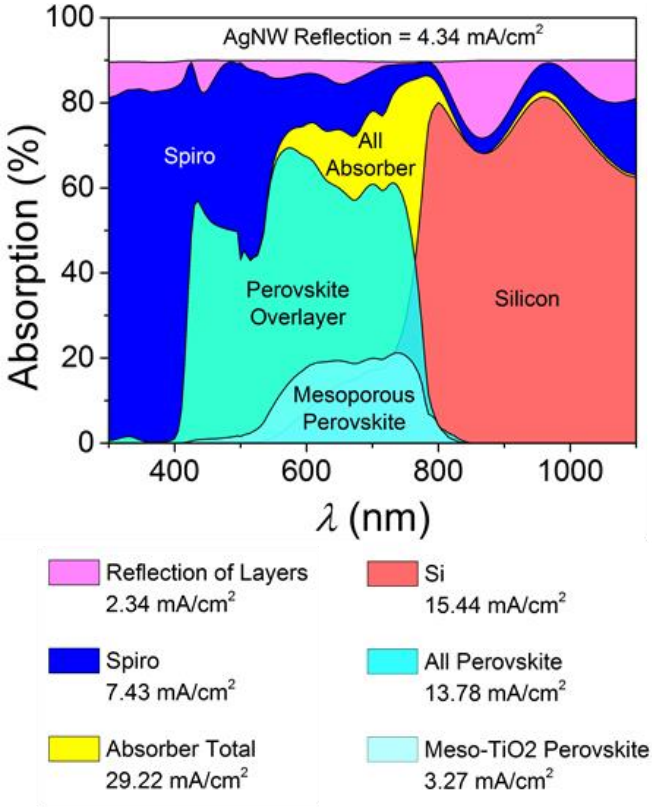

Fig. 3. Optical absorption within the different perovskite/silicon tandem layer stack simulated using FDTD.

We quantitatively analyze the optical loss within each layer in the tandem stack by using 1-D finite-difference-time-domain (FDTD) optical simulation as shown in Fig. 3. The refractive index of the mesoporous perovskite layer is modeled as the volume-weighted-average of the TiO_2 and perovskite (32% and 68%, respectively) refractive index in the mesoporous layer. The optical absorption within each layer is integrated under the AM1.5G spectrum, and we show that the largest optical loss happens in the Spiro-OmeTAD layer, which is equivalent to a J_{SC} loss of 7.4 mA/cm^2. We further show that the total integrated optical absorption within the perovskite layer is equivalent to a J_{SC} of 13.8 mA/cm^2. This simulated absorption is quite larger than the measured J_{SC} of 11.5 mA/cm^2, indicating that the carrier collection within the perovskite overlayer is slightly inefficient. When the optical absorption plot is compared with the measured *EQE* [2], we can immediately see that the *EQE* is lower at wavelengths shorter than 600 nm. Photons with these wavelengths are strongly absorbed by the perovskite overlayer; this means that some of the free electrons generated within the perovskite overlayer close to the perovskite/Spiro-OMeTAD interface are unable to reach the TiO_2 electron selective contact and enter the tunnel junction before recombining. Finally, we also see that the *EQE* in the bottom silicon cell is much lower than the simulated optical absorption for λ = 1000–1100 nm, indicating that the silicon cell has large rear surface recombination. In order to make better perovskite/silicon tandem cell, we need to reduce Spiro-OMeTAD parasitic absorption, increase the carrier collection efficiency within the perovskite overlayer, and reduce the silicon cell's rear surface recombination.

III. Conclusion and Outlook

In summary, we report the demonstration of a monolithic perovskite/silicon tandem solar cell, enabled by a silicon-based tunnel junction as the recombination interlayer. While the V_{OC} of the device (1.58 V) is within expectation, the efficiency of the tandem cell (η = 13.7%) is low because the cell is severely current-limited by the top perovskite cell. Further innovation on finding spiro-OMeTAD replacements (reduce parasitic absorption) and increasing carrier collection efficiency in the perovskite overlayer region will be crucial to improve the monolithic tandem efficiency in future iterations of the device. Reduction in the rear surface recombination of our bottom silicon cell will also be necessary.

References

[1] C. D. Bailie, M. G. Christoforo, J. P. Mailoa, A. R. Bowring, E. L. Unger, W. H. Nguyen, J. Burschka, N. Pellet, J. Z. Lee, M. Grätzel, R. Noufi, T. Buonassisi, A. Salleo, M. D. McGehee, "Semi-transparent Perovskite Solar Cells for Tandems with Silicon and CIGS," *Energy & Environmental Science*, vol. 8, pp. 956-963, 2015.

[2] J.P. Mailoa, C.D. Bailie, E.C. Johlin, E.T. Hoke, A.J. Akey, W.H. Nguyen, M.D. McGehee, T. Buonassisi, "A 2-terminal perovskite/silicon multijunction solar cell enabled by a silicon tunnel junction," *Applied Physics Letters*, vol. 106, p. 121105, 2015.

[3] D. Gebeyehu, C. J. Brabec, N. S. Sariciftci, D. Vangeneugden, R. Kiebooms, D. Vanderzande, F. Kienberger, H. Schindler, "Hybrid solar cells based on dye-sensitized nanoporous TiO_2 electrodes and conjugated polymers as hole transport materials," in *Synthetic Metals*, vol. 125, pp. 279-287, 2002.

[4] N. J. Jeon, J. H. Noh, Y. C. Kim, W. S. Yang, S. Ryu, S. I. Seok, "Solvent engineering for high-performance inorganic–organic hybrid perovskite solar cells," in *Nature Materials*, vol. 13, pp. 897-903, 2014.